AIAA JOURNAL
Vol. 30, No. 12, December 1992

Effect of Modal Interaction on Sound Radiation from Vibrating Structures

Kenneth A. Cunefare*
Georgia Institute of Technology, Atlanta, Georgia 30332

When a structure responds such that multiple modes are contributing to the total vibration and are therefore contributing to the total radiated acoustic power, it is difficult to assess which modes are contributing significantly to the sound power. For harmonic response about and above the coincidence wave number, the mode dominating the vibration response may not be the mode dominating the acoustic response. In addition, the structural modes in general do not radiate independently, such that a portion of the radiated power is attributable to acoustic interaction between modes. The research presented here develops analytical and computational tools to assess the contribution of individual modes to a structure's total radiated sound power, including interaction effects, for planar structures. Furthermore, this research presents a numerical technique for accomplishing this for structures that do not posses analytical modes. A parallel analytical and numerical development for a baffled, finite, simply-supported beam is used to illustrate the significance of the coupling and to compare the accuracy of the numerical technique against the analytical technique. A power matrix and modal power representation are employed to assess the coupling between modes and to determine the total power radiated by an individual mode, in the presence of all other modes.

Nomenclature

$\boldsymbol{C}$ = coupling coefficient matrix
C_{ij} = i, jth element of C
c = speed of sound in acoustic medium
$\boldsymbol{h}$ = vector of shape functions
$J(\eta)$ = Jacobian of coordinate transformation
k = acoustic wave number, ω/c
k_n = structural wave number of nth mode, $n\pi/l$
l, w = length and width of beam
l_e = length of an element in discretized beam
N = number of elements in numerical model
R = distance between source point x and observation point r, $|x - r|$
r, θ, ϕ = spherical coordinates
$\boldsymbol{u}$ = vector of modal amplitude coefficients, u_n
$u(x)$ = velocity distribution along length of beam
v = surface normal velocity
$\boldsymbol{v}$ = vector of nodal velocities (v, θ)
W = total acoustic power
W_i = acoustic power radiated by ith mode, including interaction effects
α = $kl \sin(\theta) \cos(\varphi)$
β = $kw \sin(\theta) \sin(\varphi)$
η = natural coordinate
θ = gradient of surface normal velocity
ρ = density of acoustic medium
σ = acoustic radiation efficiency
$\phi(x)$ = vector of eigenfunctions
Ψ = matrix of numerically derived eigenvectors, ψ
ω = acoustic frequency, rad/s

Introduction

WHEN a structure is responding harmonically such that multiple structural modes are contributing to the surface motion, it is difficult to assess the relative importance of each individual mode's contribution to the total radiated sound power. Below the coincidence wave-number ratio, defined as $k/k_n = 1$, the radiation efficiencies of individual modes, considered in the absence of all other modes, may vary by many orders of magnitude for a given response frequency. The mode dominating the vibration response may not be the mode dominating the acoustic response. Furthermore, the modes do not in general radiate independently of one another. That is, the total radiated sound power includes contributions from each individual mode, plus contributions due to the interaction of each mode with all other modes. Therefore, the individual mode's radiation efficiencies may not be an accurate measure of the significance of individual modes in multimodal response. The research presented in this paper addresses these issues by presenting techniques for assessing the relative contributions of individual structural modes, including their interaction with all other modes. Furthermore, this paper presents a technique for accomplishing this task for structures whose surface motion cannot be expressed in terms of analytical modes, but where the modes are determined through numerical techniques, such as the finite element method.

Past work in addressing modal coupling has generally focused on specific excitations or fluid loading. Skudrzyk[1] pointed out that, for a plate with multiple modes present, the total radiated acoustic power would not be the sum of the powers from individual modes due to the presence of coupling effects. Reddy[2] considered random acoustic excitation, whereas Davies[3,4] considered random excitation with heavy fluid loading. Both Reddy and Davies considered the radiation from plates. Yousri and Fahy[5] examined the intermodal coupling for infinite unbaffled cylindrical beams.

Recently, Keltie and Peng[6] presented a more general technique to determine the coupling between modes on a baffled one-dimensional beam. Keltie and Peng expressed the coupling in terms of a power radiation coefficient. The power radiation coefficient represents a weighting factor between particular modes, independent of amplitude. This power radiation coefficient multiplied by the product of the amplitudes of two modes yields a product directly proportional to the power radiated due to the interaction between the modes. Keltie and Peng observed that the intermodal coupling, represented by the power radiation coefficients, is significant below the coincidence wave number ratio. As evidenced by the work of Wallace[7] and Levine,[8] the radiation efficiencies of the

Received Nov. 21, 1991; presented as Paper 92-0372 at the AIAA 30th Aerospace Sciences Meeting, Reno, NV, Jan. 6-9, 1992; revision received May 19, 1992; accepted for publication May 26, 1992.

*Assistant Professor, Department of Mechanical Engineering.

modes on baffled simply-supported uniform beams approaches unity well above the coincidence wave number ratio. This work, coupled with that of Davies[3,4] and Keltie and Peng,[6] implies that well above the coincidence wave number ratio the interaction between modes is negligible and that the radiation from individual modes can be treated independently from all other modes. Therefore, the work presented in this paper is applicable in the near coincidence and below coincidence wave number ratio regimes.

The issue of coupled modes with respect to acoustic radiation impacts the acoustic design of structures, the acoustic analysis of existing structures, and the design and analysis of active structural acoustic control (ASAC) systems, among other areas. From the standpoint of acoustic design, current numerical modeling techniques, such as the acoustic boundary element method, cannot resolve individual modal contributions and interactions, since they deal with total velocities on the surface of a structure. But since the total velocities are used in the formulations, the modal contributions and interactions are properly accounted for. And yet such fine detail on the modal radiation would be of interest to a designer by providing information that would enable greater control over the acoustic characteristics of the final design. The same comment applies to the analysis of the acoustic radiation from existing structures: Current modeling techniques cannot resolve individual and interaction contributions to the total radiated sound power. Passive noise control methods applicable to such structures would benefit from a clear understanding of modal contributions and interactions by permitting the tailoring of the methods to only the dominant modes.

The issue of coupled modes has particular impact on the design of active noise control (ANC) systems and ASAC systems. For classical ANC systems the secondary control sources need to be located within one-quarter wavelength of the antinodes of the radiating modes.[9] For a multimodal structure this requires identification of the dominant modes. For ASAC systems, which use direct force or moment inputs to a structure to control the overall vibration response, explicitly identifying the strongly radiating and strongly coupled modes may simplify the design of such systems, by reducing the number of controlled modes and hence reducing the number of sensors and actuators.

Intermodal coupling has recently been treated by researchers in ASAC systems. ASAC systems generally use the minimization of the radiated acoustic power as the objective function. Thus, this objective function will incorporate the intermodal coupling effects. Although this control approach properly accounts for individual and mutual interaction contributions to the total radiated sound power, little *explicit* use has been made of the coupling interaction information in the design of control systems, for example, through the identification and selection of which modes to control.

Baumann et al.[10] considered the control of impulsively excited structures, using both minimal vibration and minimal acoustic radiation (ASAC) as control objectives. For the ASAC system they derived a coupling matrix that they interpreted in terms of self- and mutual radiation efficiencies of the structural modes. Pan et al.[11] presented a general derivation and discussion for the control of the acoustic radiation from a multimodal rectangular panel. In fact, the work by Pan et al. uses many of the same concepts employed here, in terms of expanding velocities in terms of modes and combining that expansion with a radiation model. However, their minimal power objective function is expressed in terms of control forces, such that the individual and interaction modal contributions, although properly accounted for, are not readily identifiable. Neither Baumann et al. nor Pan et al. use explicit coupling information to assist in the design of their control implementations; however, it must be re-emphasized that the interactions are properly accounted for in their respective objective functions. Fuller and Burdisso[12] derived an ASAC control law based on a wave-number approach. Their control law effectively incorporates wave-number transforms of the self and mutual interactions. But again, the potential usefulness of such information in identifying the dominant modes, or strongly coupled modes, is not addressed. A number of other works reflecting ASAC research[13-18] has appeared that incorporate coupling information in the control objective functions, but do not exploit it in the physical design of the control implementations.

The following sections develop the analysis techniques necessary for assessing the relative contributions of individual modes to the total multimodal radiated sound power. The development begins with an analytical approach for the determination of intermodal coupling for finite beams. This analysis represents an extension to that employed by Wallace[7] and leads to an interpretation of the intermodal coupling in terms of self and mutual radiation efficiencies. The analytical development and the intermodal coupling development are presented somewhat briefly, since this work is similar to that performed by other authors. The technical presentation then focuses on developing a method for determining intermodal coupling information for structures that do not have analytical modes. Both the analytical and numerical developments will use the example of a simply-supported finite beam as a basis for comparison between them. Since both the analytically and numerically derived coupling information is independent of any specific excitation or modal response, the subsequent section presents tools for converting the coupling information into more directly useful forms. Finally, computational examples comparing the analytical development to the numerical development complete the technical portion of the paper.

Analytical Procedure for a Simply-Supported Uniform Beam

Consider the baffled, simply-supported uniform beam of length l and width w depicted in Fig. 1. The beam is assumed to be undergoing forced response at a frequency ω, such that multiple modes are present in the velocity response spectrum. The material details of the beam's composition can be neglected at this point, since the mode shapes will be independent of the properties (for a uniform beam).

Surface Velocity Distribution

For a lightly damped or undamped simply-supported beam in harmonic motion at a single frequency, the surface velocity distribution can be represented by a series expansion in terms of the eigenfunctions, or modes of the beam, such that

$$u(x) = \boldsymbol{u}^T \boldsymbol{\phi}(x) \tag{1}$$

where $\boldsymbol{u}$ represents a vector of known modal amplitude coefficients, u_n; $\boldsymbol{\phi}(x)$ represents a vector of the corresponding mode shapes (eigenfunctions); and the harmonic time dependence has been neglected. The mode shapes for the simply-supported beam are of the form $\sin(k_n x)$, where $k_n = n\pi/l$ represents the structural wave number of the nth mode. In Eq. (1) the

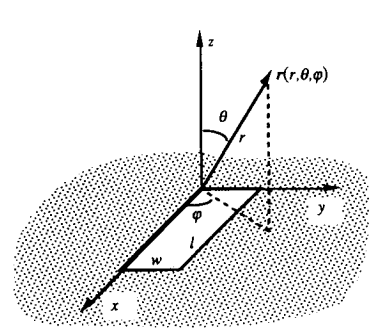

Fig. 1 Simply-supported beam in an infinite rigid baffle.

vectors $\boldsymbol{u}$ and $\boldsymbol{\phi}$ have dimensions equal to the chosen length of the expansion. The surface velocity is assumed to be uniform across the width of the beam.

Far-Field Acoustic Pressure

Radiation is considered only into the half-space defined by $+z$. Assuming that the medium in contact with the beam is a light fluid, then fluid loading of the beam can be neglected. The Rayleigh integral[19] will be used to model the radiation from the beam. This restricts the following development to planar geometries. Through the use of the Rayleigh integral, the pressure at a point $r(r, \theta, \phi)$ in the far field can be expressed as

$$p(r) = -ik\rho c \frac{e^{ikr}}{2\pi r} \int_0^w \int_0^l u(x) \exp\left\{-i\left[\alpha\left(\frac{x}{l}\right) + \beta\left(\frac{y}{w}\right)\right]\right\} dx\, dy \tag{2}$$

Using Eq. (1) in Eq. (2) and integrating each resulting term yields

$$p(r) = \frac{\rho c w}{\pi} \boldsymbol{u}^T \boldsymbol{b}(r) \tag{3}$$

where $\boldsymbol{b}$ represents a vector composed of terms of the form

$$b_n(r) = -\frac{k}{k_n} \frac{e^{ikr}}{2r} \left(\frac{1 - (1)^n e^{-i\alpha}}{1 - (\alpha/n\pi)^2}\right)\left(\frac{1 - e^{-i\beta}}{\beta}\right) \tag{4}$$

Radiated Acoustic Power

The integral over a hemisphere in the far field of the average acoustic intensity yields the total acoustic power radiated by the beam:

$$W = \int_0^{2\pi} \int_0^{\pi/2} \frac{|p(r)|^2}{2\rho c} r^2 \sin(\theta)\, d\theta\, d\varphi \tag{5}$$

Using Eq. (3) in Eq. (5) leads to

$$W = \rho c w^2 \boldsymbol{u}^H \boldsymbol{C} \boldsymbol{u} \tag{6}$$

where the superscript H in Eq. (6) represents the Hermitian of the vector (complex conjugate transpose). $\boldsymbol{C}$ represents a strictly real matrix of integrals of the form

$$C_{mn} = \frac{1}{2\pi^2} \int_0^{2\pi} \int_0^{\pi/2} b_m^*(r) b_n(r) r^2 \sin(\theta)\, d\theta\, d\varphi \tag{7}$$

Using Eq. (4) in Eq. (7) and evaluating the resulting integrands leads to the result that the odd and even modes are decoupled[3,4,6,20] for the simply-supported beam. That is, the odd and even modes are independent of each other, but the odd modes are not independent of other odd modes, and similarly for the even modes. This decoupling can be seen by expanding the matrix representation for the radiated power as

$$W = \rho c w^2 \boldsymbol{u}^H \begin{bmatrix} C_{11} & 0 & C_{13} & 0 & \cdots \\ 0 & C_{22} & 0 & C_{24} & \\ C_{31} & 0 & C_{33} & 0 & \\ 0 & C_{42} & 0 & C_{44} & \\ \vdots & & & & \ddots \end{bmatrix} \boldsymbol{u} \tag{8}$$

Equation (8) clearly implies that the powers radiated by the even-even modes and the power radiated by the odd-odd modes are independent of each other. It should be emphasized that "decoupled" is used in the sense that the odd and even modes do not interact with one another with respect to the total radiated sound power. Furthermore, note that the coupling matrix $\boldsymbol{C}$ is independent of the magnitude of the modes themselves. $\boldsymbol{C}$ simply weights the interaction between individual modes.

If a mode's wave number ratio is above the coincidence wave number ratio (i.e., $k/k_n = kl/n\pi > 1$), then the off-diagonal elements associated with that mode become small compared to the diagonal element. The off-diagonal elements do not go to identically zero, as pointed out by Levine,[8] but are negligible compared to the diagonal elements. This condition implies that the modes radiate essentially independently and can be treated individually.

Radiation Efficiency and Coupling Coefficients

The interpretation of the elements of $\boldsymbol{C}$ can be elucidated by examining the radiation efficiency of the simply supported beam. The radiation efficiency is defined as

$$\sigma = \frac{W}{\rho c w l \langle |u(x)|^2 \rangle} \tag{9}$$

where $\langle |u(x)|^2 \rangle$ represents the spatial mean square velocity. For sinusoidal components the spatial mean square velocity is simply one-fourth the magnitude of the modal amplitude vector, $\langle |u(x)|^2 \rangle = \boldsymbol{u}^H \boldsymbol{u}/4$, such that with Eq. (6) the radiation efficiency is

$$\sigma = \frac{4w}{l} \frac{\boldsymbol{u}^H \boldsymbol{C} \boldsymbol{u}}{\boldsymbol{u}^H \boldsymbol{u}} \tag{10}$$

Now consider Eq. (10), for $w/l = 1.0$, and for the first mode only. Then

$$\sigma = \frac{4u_1^* C_{11} u_1}{u_1^* u_1} = 4C_{11} \tag{11}$$

Equation (11) implies that the elements of $\boldsymbol{C}$ represent one-fourth the magnitude of the radiation efficiencies for the modes of a beam with an aspect ratio w/l equal to unity. The terms on the diagonal C_{mm} are directly proportional to the self-radiation efficiency of the mth mode independent of all other modes. The off-diagonal terms C_{mn} are directly proportional to the mutual radiation efficiencies of the interaction between the mth and nth modes. The matrix $\boldsymbol{C}$ completely defines the coupling between the modes on the beam, including the coupling of a given mode to itself.

Now consider the power radiated by the first and third modes, again for $w/l = 1.0$. Through Eq. (6), and taking advantage of the symmetry of $\boldsymbol{C}$,

$$W = \rho c w^2 [|u_1|^2 C_{11} + |u_3|^2 C_{33} + 2C_{13} \mathrm{Re}(u_1^* u_3)] \tag{12}$$

which clearly indicates that the total intermodal coupling coefficient is twice that of a single off-diagonal element of $\boldsymbol{C}$.

Long Wavelength Approximation to Coupling Coefficients

For acoustic wavelengths that are long compared to the length of the beam (i.e., for $kl/\pi \ll 1$), it is possible to obtain accurate first-order approximations to the elements of $\boldsymbol{C}$. This is accomplished by expanding Eq. (4) in a Taylor series in terms of kl/π and neglecting higher-order terms. This yields a first-order approximation to b_n in terms of a general index n. C_{mn} is then obtained by using this approximation in the integration indicated by Eq. (7). Wallace[7] employed this technique for determining the radiation efficiencies for individual modes (i.e., for C_{mm}). The following results were obtained by the same process as that used by Wallace, but extending it to account for interactions between modes m and n. For odd components this procedure yields

$$C_{mn} \approx \frac{1}{\pi} \frac{w}{l} \left(\frac{k^2 l^2}{mn\pi^2}\right) = \frac{C_0}{mn} \tag{13}$$

where the constant C_0 has been introduced for compactness. For even components this procedure yields

$$C_{mn} \approx \frac{\pi_{mn}}{12}\frac{w}{l}\left(\frac{k^2l^2}{mn\pi^2}\right)^2 = \frac{C_e}{mn} \tag{14}$$

where the constant C_e has been introduced for compactness.

Equation (13) implies that the largest coupling coefficient is C_{11} for the odd components, whereas Eq. (14) implies that C_{22} is the largest for the even components (C_{12} and C_{21} are both identically zero, since the odd and even modes are decoupled). Equations (13) and (14) together imply that the coupling coefficients decrease with increasing mode number. Equations (13) and (14) also imply that the radiation efficiencies of succeeding individual modes go as the inverse of the square of the mode number, since C_{nn} is directly proportional to the radiation efficiency of the nth mode.

Recall that C represents a matrix of weighting factors between modes with respect to the total radiated power. It is informative to compare the elements of C to one another, because this provides quantitative information regarding how well the modes couple to one another. Although it is possible to form comparative ratios between coupling coefficients for odd modes and even modes, this does not provide much useful information, since the odd and even modes are decoupled.

The ratio C_{mn}/C_{mm} represents a measure of the magnitude of the coupling coefficient between modes m and n to the magnitude of the coupling coefficient of the mth mode to itself. Equivalently, C_{mn}/C_{mm} represents the ratio between the mutual radiation efficiency between modes m and n to the radiation efficiency of mode m alone. For both the odd and even components this ratio is

$$C_{mn}/C_{mm} \approx m/n \tag{15}$$

where both m and n must be odd or even.

For fixed m and for $m < n$, Eq. (15) implies that the coupling between modes decreases with increasing modal separation (increasing n). Equation (15) also implies that, for $m > n$, the coupling interaction between the mth and nth modes is greater than that of the mth mode to itself. For a given mode m, then, the coupling interaction decreases between mode m and higher modes n, relative to the coupling interaction of mode m to itself, while the magnitude of the interaction between mode m and higher modes n will always be less than the coupling interaction of mode m to itself. Similarly, for a given mode m the coupling interaction increases between mode m and lower modes n, relative to the coupling interaction of mode m to itself, while the magnitude of the interaction between mode m and lower modes n will always be greater than the coupling interaction of mode m to itself. This last statement has the direct consequence that the power radiated due to the coupling interaction between a higher mode and a lower mode can be significantly greater than power radiated by the higher mode alone.

The quantity C_{nn}/C_{mm} represents the ratio between the coupling coefficient of mode n to itself and the coupling coefficient of mode m to itself. Equivalently, it represents the ratios between the self radiation efficiencies of modes n and m. For both the odd and even components this ratio is

$$\frac{C_{nn}}{C_{mm}} \approx \frac{m^2}{n^2} \tag{16}$$

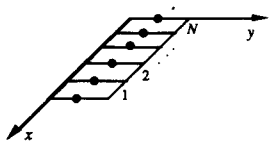

Fig. 2 Beam divided into N elements.

where, again, both m and n must be odd or even. Equation (16) clearly indicates that the radiation efficiencies of individual modes, for the long wavelength condition employed here, can vary by many orders of magnitude.

Again, it must be emphasized that the modal coupling coefficients are independent of specific modal amplitudes. With respect to the power radiated by interactions between modes, the modal coupling coefficients are the weighting factors between modes.

Procedure for Structures Without Analytical Modes

The method described previously is applicable to structures with known analytical modes. However, it is not suitable for structures without analytical modes. Such structures are commonly analyzed through the use of numerical methods, such as the finite element method or the boundary element method. Numerical models of the acoustic radiation are generally formulated in terms of the total surface normal velocity, such that modal velocity contributions cannot be resolved. The following development shows how modal coupling data can be extracted from such numerical analyses. The following development, up to the expression for radiated power in terms of total velocities, is an adaptation of the development presented by Naghshineh.[21]

Numerical Approximation for Surface Quantities

Consider the baffled finite beam of length l and width w depicted in Fig. 1. Again, radiation is considered only into the half-space defined by $+z$, the surface velocity is assumed to be uniform across the width of the beam, and fluid loading is neglected. For the purposes of numerical approximations, the surface of the beam is subdivided into N elements, as shown in Fig. 2, with each element defined by two nodes. Through the use of interpolation functions, or shape functions, the acoustic pressure or surface velocity anywhere within an element can be approximately calculated based on values at the nodes of the element. Functionally, this can be represented as

$$f(x) = h_1(x)f_1 + h_2(x)f_2 + \cdots = \boldsymbol{h}^T(x)\boldsymbol{f} \tag{17}$$

where the h_1, h_2, etc., are interpolation functions, and the f_1, f_2, etc., are values of the function $f(x)$ at the nodes of the element. The specific forms of the interpolation functions h and the values f depend on the particular interpolation scheme selected, such as constant, linear, or quadratic.

For the work presented in this paper, cubic Hermitian shape functions, represented by

$$\boldsymbol{h}^T(\eta) = \{h_1(\eta),\ h_2(\eta),\ h_3(\eta),\ h_4(\eta)\}$$

and defined as

$$\boldsymbol{h}^T(\eta) = \{\tfrac{1}{4}(1-\eta)^2(2+\eta),\ l_e/8(1-\eta)^2(\eta+1)$$
$$\tfrac{1}{4}(1+\eta)^2(2-\eta),\ l_e/8(1+\eta)^2(\eta-1)\} \tag{18}$$

are used to map the velocity distribution across each element.[22] The cubic Hermitian shape functions were selected since they preserve the continuity of the surface normal velocity and its gradient across element boundaries. In Eq. (18) l_e represents the length of the particular element to which these shape functions are applied. Figure 3 depicts the form of these functions with respect to η, for $l_e = 1$, where η represents a natural coordinate that varies between -1 and $+1$. The use of the natural coordinate η simplifies the task of numerical integration, since the domain of integration is always -1 to $+1$; hence, only a single integration rule is necessary. However, the complication to using this approach is that the spatial variable x within an element j must be mapped to the natural coordinate by

$$\eta = [2(x - x_j)/l_e] - 1 \tag{19}$$

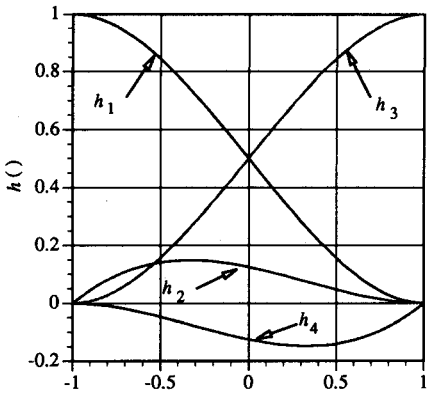

Fig. 3 Cubic Hermitian shape functions.

Cubic Hermitian shape functions operate on the values of an interpolant and its gradient at the nodes defining a given element to generate values at points within the element. Therefore, to interpolate the velocity distribution across the jth element, the shape functions operate on the normal velocities v and on the gradient of the normal velocity θ at the nodes defining the end points of the element. For each element, these nodal velocities and gradient are represented in a vector form as

$$v_j^T = \{v_j, \theta_j, v_{j+1}, \theta_{j+1}\} \tag{20}$$

The velocity at a point x within the jth element is then determined by

$$v[\eta(x)] = \boldsymbol{h}_j^T[\eta(x)]v_j \tag{21}$$

Since each node has two degrees of freedom (velocity and gradient of velocity), the total degrees of freedom is equal to twice the total number of nodes in the model. Collecting all of the $\boldsymbol{h}_j$ vectors into a single vector $\boldsymbol{h}$ and all of the velocity vectors v_j into a single vector v yields

$$v[\eta(x)] = \boldsymbol{h}^T[\eta(x)]v \tag{22}$$

for the velocity distribution anywhere along the length of the beam.

Numerical Approximation for Pressure

As with the development for structures with analytical modes, the Rayleigh integral will be used to obtain an expression for the acoustic pressure. However, the integral will be formulated in terms of the surface pressure, instead of using a far-field form of the integral. Without analytical modes there is no particular advantage to using a far-field integral. For the pressure at a point r on the surface of the beam, the Rayleigh integral yields

$$p(r) = -ik\rho cw\int_0^l v(x)\frac{e^{-ikR}}{2\pi R}\,dx \tag{23}$$

For each element on the beam (i.e., the jth element), the use of Eq. (21) in Eq. (23) will yield four integrals, one for each shape function, or

$$b_{\alpha j}(r) = -ik\int_{-1}^{+1} h_{\alpha j}(\eta)\frac{e^{-ikR(\eta)}}{2\pi R(\eta)}J(\eta)\,d\eta, \quad \alpha = 1, 2, 3, 4 \tag{24}$$

In Eq. (24), $J(\eta)$ represents the Jacobian of the transformation, Eq. (21). Note that the elements of v_j have not been included in the definition of $b_{\alpha j}$ since they are not a function of the integration variable. Combining the results of Eq. (24) into a vector permits the pressure at r due to the velocity distribution on the jth element to be represented as

$$p_j(r) = \rho cwv_j^T\boldsymbol{b}_j(r) \tag{25}$$

Repeating this process for all N elements in the model yields

$$p(r) = \rho cw[v_1^T\boldsymbol{b}_1(r) + v_2^T\boldsymbol{b}_2(r) + \cdots + v_N^T\boldsymbol{b}_N(r)] \tag{26}$$

or

$$p(r) = \rho cwv^T\boldsymbol{b}(r) \tag{27}$$

where the subvectors v_j and $\boldsymbol{b}_j$ have been assembled into global matrices v and $\boldsymbol{b}$, respectively. Note that at this point the integrals in $\boldsymbol{b}$ have not been evaluated, since they would be undefined as a consequence of the singularity at $r = x$. A more rigorous development of this point is presented by Naghshineh,[21] although the aforementioned development is adequate for the purposes here.

Numerical Approximation for Radiated Power

As with the development for structures with analytical modes, an intensity integration will be used to obtain an expression for the total radiated power. However, the integral will be formulated in terms of the surface intensity, instead of using a far-field form. Indeed, a far-field formulation may actually lead to a more computational intensive integration than a surface integration, due to the necessity of adequately sampling the far field. Taking the real part of the surface intensity integral yields the radiated power,

$$W = \frac{1}{2}\,\mathrm{Re}\left\{\int_0^w\int_0^l p(x)v^*(x)\,dx\,dy\right\} \tag{28}$$

The pressure and velocity in Eq. (28) can be replaced with Eqs. (27) and (22), respectively, yielding

$$W = \rho cw^2\int_0^l v^T\boldsymbol{b}(x)[\boldsymbol{h}^T(x)v]^*\,dx \tag{29}$$

or

$$W = \rho cw^2v^H\boldsymbol{B}v \tag{30}$$

where the elements of $\boldsymbol{B}$ are found from

$$B_{mn} = \frac{1}{2}\,\mathrm{Re}\left\{\int_0^l \boldsymbol{b}_m^T(x)\boldsymbol{h}_n^*(x)\,dx\right\} \tag{31}$$

Recall that the elements of $\boldsymbol{b}$ were not evaluated due to a singularity at $r = x$. The same singularity exists in Eq. (31). But since only the real component of Eq. (31) is retained, the singular function reduces to $\sin kR/kR$ as $kR \to 0$, which possesses a finite limit. As for the pressure and velocity integrations, the global variables x in the power integration has to be mapped to the local coordinate η on each element.

Note that Eq. (30) has the same form as Eq. (6). However, where Eq. (6) is expressed in terms of modal amplitude coefficients $\boldsymbol{u}$, Eq. (30) is expressed in terms of total nodal velocities v.

Extraction of Modal Coupling from Numerical Approximations

Extracting modal coupling information from the matrix $\boldsymbol{B}$ requires expressing the nodal velocities through a modal expansion. Through standard finite element analysis techniques[22] the equations of motion for the beam can be expressed as

$$[\boldsymbol{K} - \omega^2\boldsymbol{M}]\psi = 0 \tag{32}$$

where $\boldsymbol{K}$ and $\boldsymbol{M}$ are global mass and stiffness matrices, respectively, and ψ and ω are the natural mode shape vector and its

corresponding natural frequency, respectively. Note that this model does not include damping. K and M must be obtained by use of the same element mapping as that used to obtain Eq. (30). This ensures that the degrees of freedom considered in the structural analysis coincide identically with the degrees of freedom considered in the acoustic radiation analysis.

The solution of the eigenvalue problem posed by Eq. (32) yields a vector of natural frequencies Λ and a matrix of real valued eigenvectors (mode shapes) Ψ. Note that the eigenvectors are defined with respect to nodal displacements and gradients for the same nodes as those used for the acoustic radiation analysis. The number of mode shapes ψ determined through Eq. (32) is equal to the number of degrees of freedom used to model the structure. However, the higher-order mode shapes and eigenvalues are not as accurate as the lower modes. Indeed, only half of the eigenvalues can be considered to be reliable in general,[23] and since the eigenvalues are more accurate than the eigenvectors, only half of the eigenvectors can be considered to be reliable. The higher modes are therefore neglected when the response of a structure is modeled and, as such, should also be eliminated from the radiation model.

For the cubic Hermitian elements used here, the number of degrees of freedom in the model depends on the number of elements in the model N such that DOF = $2N + 2$. Eliminating DOF $- R$ high-order modes leaves a series expansion of length R and reduces the dimension of Ψ from DOF $\times$ DOF to DOF $\times R$. Note that B has dimension DOF $\times$ DOF. Normalizing the reduced set of eigenvectors such that $\Psi^T\Psi = I$, where I represents the identity matrix, then for any arbitrary velocity distribution, defined in terms of nodal velocities, the expansion theorem can be used to express this distribution in terms of the natural modes. That is,

$$v(x) = \sum_{n=1}^{R} u_n \psi_n(x) \tag{33}$$

or

$$v = \Psi u \tag{34}$$

In Eq. (34), v represents any arbitrary velocity distribution defined at the nodes, and u represents modal participation coefficients. Using Eq. (34) in Eq. (30) yields

$$W = \rho c w^2 u^H \Psi^H B \Psi u \tag{35}$$

Defining $\Psi^T B \Psi = C$, then Eq. (35) becomes

$$W = \rho c w^2 u^H C u \tag{36}$$

where C in Eq. (36) now has the exact same interpretation and significance as the matrix C obtained through the analytical development. That is, the elements of C represent the coupling between the modes. Recall that C was obtained through the use of a reduced set of eigenvectors and has dimension $R \times R$.

Power Matrix

Finally, a powerful technique for visualizing the coupling for a particular problem involves the generation and manipulation of a "power matrix," obtained from Eq. (6) or Eq. (36). This matrix is obtained by carrying through the vector and matrix multiplications and representing the resulting products in matrix form, or

$$W = \rho c w^2 W$$

$$= \rho c w^2 \begin{bmatrix} C_{11}u_1^*u_1 & 0 & C_{13}u_1^*u_3 & 0 & \cdots \\ 0 & C_{22}u_2^*u_2 & 0 & C_{24}u_2^*u_4 & \\ C_{31}u_3^*u_1 & 0 & C_{33}u_3^*u_3 & 0 & \\ 0 & C_{42}u_4^*u_2 & 0 & C_{44}u_4^*u_4 & \\ \vdots & & & & \ddots \end{bmatrix} \tag{37}$$

where it is understood that the sum of the elements in Eq. (37), multiplied by the leading coefficient, yields the total power. Each element W_{mn} in Eq. (37) is proportional to the total power radiated due to an individual mode ($m = n$), or due to acoustic modal interaction ($m \neq n$). Comparing the relative magnitudes of these elements clearly identifies the modes that are most important as far as contributions to the total radiated power is concerned.

It is possible, using Eq. (37), to assess the total contribution to the radiated acoustic power due to a single mode, including all interaction effects. The modal power W_i, representing the total radiated power attributable to the single mode i in the presence of all other modes, is given by

$$W_i = \rho c w^2 \left[C_{ii}u_i^*u_i + \sum_{\substack{j=1 \\ j\neq i}}^{R} C_{ij}u_j^*u_i + \sum_{\substack{j=1 \\ j\neq i}}^{R} C_{ji}u_i^*u_j \right] \tag{38}$$

which is simply the sum across the ith row and down the ith column, but counting the diagonal element only once. This procedure accounts for all interactions of the ith mode with all other modes, including with itself. Note that the sum of all the modal powers in a given analysis will be greater than the total power radiated by the structure, due to double counting of the mutual interaction powers. In fact, since the diagonal elements are counted only once, the sum of the modal powers will differ from twice the total power by the sum of the diagonal elements, or

$$\sum_{i=1}^{R} W_i = 2W - \sum_{i=1}^{R} C_{ii}u_i^*u_i \tag{39}$$

As an interesting side development, from the structure of the power matrix (37) and of the modal power equation (38), it is evident that the sensitivity[24,25] of the total radiated power to a change in the ith velocity component is the same as the sensitivity of the ith modal power, that is,

$$\frac{\partial W}{\partial u_i} = \frac{\partial W_i}{\partial u_i} = \rho c w^2 \sum_{j=1}^{R} C_{ij}u_j^* \tag{40}$$

The power matrix is an analysis tool applicable to a given state of modal response. It is applicable to the design analysis of structures, the analysis of existing structures, and the analysis and design of active noise control systems. Current structural modeling and acoustic modeling methods permit analysts to predict the response of a given design to excitations. From the power matrix and other acoustic design tools, analysts can determine the relative acoustic advantages or disadvantages in enhancing or reducing the design response of particular structural modes. For an existing structure the power matrix and the modal powers permit the ready identification of which modes are most significant with respect to the radiated acoustic power and to identify which modes are most strongly coupled.

For the analysis and design of active structural acoustic control systems, the modal powers provide a means to make a first-order estimate of the impact of controlling particular modes on the total radiated power. For example, eliminating the ith mode from the velocity spectrum would then lead to a change in the total power by an amount W_i. Assessing the impact of eliminating multiple modes requires accounting for the fact that the summations used to compute the modal powers will include common interaction terms between the modes, such that these terms are multiply counted. For example, the modal powers for the ith and jth modes will both include $C_{ij}u_i^*u_j$ and $C_{ji}u_j^*u_i$. Therefore, estimating the power reduction from eliminating multiple modes requires summing the modal powers for the modes and then reducing the resultant quantity by a summation equal to the multiply-counted interaction terms. This procedure for estimating the effect of controlling the modal response assumes that the amplitudes of the controlled modes are reduced to zero, and no control

spillover occurs. This is not physically realizable. However, the procedure should still prove useful in the analysis and design of ASAC systems. For example, the procedure represents a means to estimate the maximum possible reduction achievable by controlling a given set of modes. Furthermore, it provides a means to perform comparative tradeoff analyses for determining how many, and which modes, to control. This holds forth the potential to reduce the complexity of ASAC systems by reducing the order and actuator count of the control system designed with this procedure over a control system that attempts to control all modes within a given model.

Numerical Results and Discussion

The results presented in this section consider the acoustic radiation from a baffled simply-supported beam. This permits the results from the numerical analysis to be directly compared to those for the analytical analysis. For the following numerical results, two FORTRAN programs were written to implement the methods described earlier. One program implemented the analytical method represented by Eqs. (1-7). The second program implemented the numerical method represented by Eqs. (17-36).

The following two subsections present two different numerical studies. The first section examines the impact of intermodal coupling on the acoustic radiation for conditions of forced excitation on the beam. The first section also presents an example of the use of the power matrix and modal power analysis techniques. The second section examines how well the numerical procedure performs compared to the analytical procedure for the determination of the coupling coefficient matrix C.

Effects of Intermodal Coupling

As a simple example, consider the acoustic radiation from a simply-supported beam, well below coincidence, with only the fist and third modes present in the vibration response. Then the total radiated power is

$$W = \rho c w^2 [|u_1|^2 C_{11} + |u_3|^2 C_{33} + 2C_{13}\,\mathrm{Re}(u_1^* u_3)] \qquad (41)$$

The relative contributions to the total radiated power can be obtained by factoring C_{11} from inside the parentheses in Eq. (41):

$$W = \rho c w^2 C_{11} \left[|u_1|^2 + |u_3|^2 \frac{C_{33}}{C_{11}} + 2\frac{C_{13}}{C_{11}}\,\mathrm{Re}(u_1^* u_3) \right] \qquad (42)$$

and then using Eq. (15) to determine the values of the coupling ratios. This yields

$$W = \rho c w^2 C_{11} \left[|u_1|^2 + |u_3|^2 \frac{1}{9} + \frac{2}{3}\,\mathrm{Re}(u_1^* u_3) \right] \qquad (43)$$

If both modes have equal amplitudes and phase, it is apparent that the first mode alone yields 56.25% of the total power, the second mode yields 6.25%, and the intermodal coupling is responsible for 37.5% of the total. Clearly, then, the intermodal coupling can not be neglected with respect to the power radiated by the individual modes.

As a second simple example, consider the same situation as the preceding, except that the first mode has only one-third the amplitude of the third mode and the same phase. Then the first mode contributes 25% of the total radiated power, the third mode 25%, and the coupling 50%. Furthermore, the first mode accounts for only 10% of the spatial average mean square velocity, whereas the third mode accounts for 90%.

Finally, consider Table 1. This table presents the power matrix and modal powers for a simply-supported beam of unit length l driven at $x/l = 0.25$ and such that $kl/\pi = 0.1$. The odd-even coupling terms have been deleted, being identically zero, to reduce clutter. The driving frequency was selected such that the flexural wave number of the excitation was near the fifth structural mode. Specifically, $k_f = 16.0$, compared to $k_s = 5\pi$. Since only relative contributions are of interest here, the modal amplitudes in Table 1 were obtained by

$$u_i = \frac{\sin(k_n x)}{k_n^4 - k_f^4} \qquad (44)$$

The modal amplitudes were then normalized such that the spatial mean square average velocity equaled unity. Because only relative contributions are of interest here, the power matrix was normalized by the total power.

Table 1 presents the interesting result that eliminating any one of the four lowest odd modes will actually increase the total radiated power, since the modal power W_i for each of these modes is negative. Examining the individual elements of the power matrix reveals that these four lowest odd modes are strongly coupled for this particular excitation. Eliminating any of the even modes from the response spectrum will have only a slight impact on the total radiated power, based on the W_i values. This illustrates the well-known fact that even modes are much less efficient radiators below coincidence than odd modes. From this power matrix and modal powers, it is possible to conclude that, for this example, only the odd modes need to be controlled, regardless of whether that control is imposed by redesigning the structure, application of passive control devices, or through application of active structural acoustic control.

Maidanik[26] demonstrated that, well below coincidence, the radiation from a given mode on a baffled finite simply-supported beam could be interpreted in terms of a monopole located at each end of the beam. The strength of each monopole is proportional to the product of the mode's amplitude and one-fourth the structural wavelength of the mode. For odd modes both monopoles have the same phase. For even modes the monopoles have opposite phase. The first mode, again well below coincidence, can be modeled as a monopole centered on the beam with strength proportional to the length of the beam and the amplitude of the first mode.

Table 1 Modal amplitudes, power matrix, and modal powers, analytical

	Mode 1	Mode 2	Mode 3	Mode 4	Mode 5	Mode 6	Mode 7	Mode 8	Mode 9	Mode 10
u_i	0.2797	0.4046	0.3175	8E-17	−3.932	0.4264	0.1087	2E-17	−0.032	−0.028
Mode 1	0.5243		0.1978		−1.47		0.029		−0.007	
Mode 2		0.0023		2E-19		0.0008		3E-20		−3E-05
Mode 3	0.1978		0.0747		−0.555		0.0109		−0.002	
Mode 4		2E-19		2E-35		7E-20		3E-36		−3E-21
Mode 5	−1.47		−0.555		4.1128		−0.081		0.0186	
Mode 6		0.0008		7E-20		0.0002		1E-20		−8E-06
Mode 7	0.029		0.0109		−0.081		0.0016		−4E-04	
Mode 8		3E-20		3E-36		1E-20		2E-37		−4E-22
Mode 9	−0.007		−0.002		0.0186		−4E-04		8E-05	
Mode 10		−3E-05		−3E-21		−8E-06		−4E-22		5E-07
W_i	−1.974	0.0039	−0.622	6E-19	−0.061	0.0018	−0.082	7E-20	0.0183	−8E-05

The relative phases of the monopoles between modes depend on the relative phases of the modes. By examining the modal amplitudes in Table 1 for the example considered here, it is apparent that the first, third, and seventh modes have relative phases opposite to that of the fifth mode. Therefore, in terms of the simple monopole model just discussed, the first, third, and seventh modes destructively interfere with the fifth mode. Elimination of any one of these modes reduces the level of destructive interference, resulting in an increase in the total radiated power.

This monopole model explains the mutual interaction as well. The model is constructed by posing a distribution of monopole sources along the entire length of the beam, one per quarter wavelength. Well below coincidence, the separation distances between the equivalent monopoles are small compared to a wavelength, such that they strongly interact, whereas adjacent monopoles of opposite sign essentially cancel, effectively leaving one uncanceled equivalent monopole source at each end of the beam. As the separation distance becomes comparable to and greater than a wavelength, the interaction becomes weaker and weaker. When the separation distance is much greater than a wavelength (acoustic wavelength much shorter than structural wavelength), the equivalent sources radiate essentially independently, such that the entire surface of the beam contributes to the radiation. This behavior is borne out by the mutual interaction terms, which approach zero for acoustic wavelengths much shorter than the structural wavelengths.

Note that the power matrix and modal power simply provide the means to assess the relative weighting, or participation, of individual modes. It is quite conceivable that for a particular excitation the analysis reveals that many of the modes have equal contributions to the total radiated sound power. Conversely, it is also quite conceivable for the analysis to reveal that only a single mode has a significant contribution to the total radiated sound power.

Comparison of Analytical and Numerical Coupling Matrices

Recall from the analytical and numerical developments that the coupling matrix $\boldsymbol{C}$ is obtained independently of any specific modal distribution. The coupling matrix simply weights the interaction between modes. Therefore, for both the analytical and numerical developments it is possible to obtain the coupling matrix $\boldsymbol{C}$ without reference to a specific excitation and to compare the results to obtain a measure of how well the numerical procedure performs.

Table 2 presents the elements of the coupling matrix $\boldsymbol{C}$ derived from the analytical development for the beam, with a wave-number ratio of $kl/\pi = 0.1$. All of the components have been normalized by C_{11}. Clearly, this matrix has the form predicted by Eq. (8), and the elements are related to one another by the ratios predicted by Eqs. (13-16).

Table 3 presents the normalized elements of the coupling matrix derived from the numerical analysis of the beam, for the same value of kl/π, using the procedure leading to Eq. (36) to generate the coupling coefficients. The beam was modeled using 10 elements, with 22 degrees of freedom. Only the lowest 10 modes were retained. A comparison of Tables 2 and 3 reveals that the magnitudes of the ratios are in good agreement for the lower modes, although some elements arising from the numerical analysis exhibit opposite signs from their counterparts in the analytical analysis. Also, the agreement between the analytical results and numerical results deteriorates with increasing mode number, such that the magnitude of the elements for mode 10 are significantly greater than the elements obtained analytically.

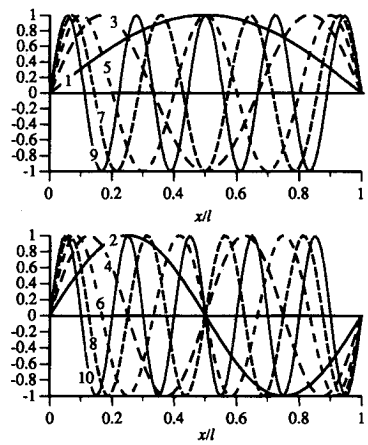

Fig. 4 Analytic mode shapes, first 10 modes: top, odd modes; bottom, even modes.

Table 2 Normalized coupling matrix using analytical method, $kl/\pi = 0.1$

	Mode 1	Mode 2	Mode 3	Mode 4	Mode 5	Mode 6	Mode 7	Mode 8	Mode 9	Mode 10
Mode 1	1.0000		0.3323		0.1994		0.1424		0.1107	
Mode 2		0.0021		0.0010		0.0007		0.0005		0.0004
Mode 3	0.3323		0.1105		0.0663		0.0473		0.0368	
Mode 4		0.0010		0.0005		0.0003		0.0003		0.0002
Mode 5	0.1994		0.0663		0.0397		0.0284		0.0221	
Mode 6		0.0007		0.0003		0.0002		0.0002		0.0001
Mode 7	0.1424		0.0473		0.0284		0.0203		0.0158	
Mode 8		0.0005		0.0003		0.0002		0.0001		0.0001
Mode 9	0.1107		0.0368		0.0221		0.0158		0.0123	
Mode 10		0.0004		0.0002		0.0001		0.0001		0.0001

Table 3 Normalized coupling matrix using numerical method, $kl/\pi = 0.1$

	Mode 1	Mode 2	Mode 3	Mode 4	Mode 5	Mode 6	Mode 7	Mode 8	Mode 9	Mode 10
Mode 1	1.0000		−0.3320		0.1975		−0.1368		0.0913	
Mode 2		0.0021		0.0010		0.0007		−0.0005		0.0072
Mode 3	−0.3320		0.1102		−0.0656		0.0454		−0.0303	
Mode 4		0.0010		0.0005		0.0003		−0.0002		0.0036
Mode 5	0.1975		−0.0656		0.0390		−0.0270		0.0180	
Mode 6		0.0007		0.0003		0.0002		−0.0002		0.0024
Mode 7	−0.1368		0.0454		−0.0270		0.0187		−0.0125	
Mode 8		−0.0005		−0.0002		−0.0002		0.0001		−0.0017
Mode 9	0.0913		−0.0303		0.0180		−0.0125		0.0083	
Mode 10		0.0072		0.0036		0.0024		−0.0017		0.0255

Table 4 Relative phase, analytical modes, and numerical modes

	Mode 1	Mode 2	Mode 3	Mode 4	Mode 5	Mode 6	Mode 7	Mode 8	Mode 9	Mode 10
Analytical	1	1	1	1	1	1	1	1	1	1
Numerical	1	−1	−1	−1	1	−1	−1	1	1	−1

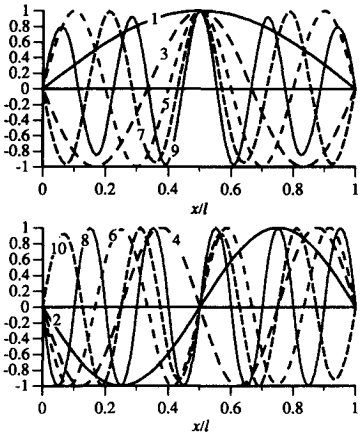

Fig. 5 Numerical mode shapes, first 10 modes: top, odd modes; bottom, even modes.

To explain the sign differences between corresponding elements in the numerically and analytically derived coupling matrices, consider Figs. 4 and 5. Figure 4 presents a plot of the analytical mode shapes of the beam as a function of distance along the length of the beam, $\psi_n(x) = \sin(k_n x)$, representing the eigenfunctions of the analytic beam response. Figure 5 presents the mode shapes obtained from the finite element analysis of the beam, representing the eigenvectors of the numerical beam response. Clearly, the phases of some of the modes determined from the finite element analysis are opposite to those used in the analytical analysis. Both the analytic eigenfunctions and the numerical eigenvectors share a common feature: They are unique only to signed constant. That is, both ψ_n and $-\psi_n$ are admissible eigenfunctions or eigenvectors. The analytical eigenfunctions all have the same positive leading constant, + 1. This establishes a certain relative phase relationship between the eigenfunctions, or modes. But what establishes the relative phasing between the numerical eigenvectors? The computational eigenvalue/eigenvector solution routine generates the eigenvectors and orthonormalizes them. This numerical representation of the eigenfunctions (i.e., the eigenvectors) defines the relative phasing.

For the example used in this paper, the sine series representation for the mode shapes represents a certain relative phasing for the modes. The numerically derived mode shapes represent another relative phasing for the modes. It is quite possible that the relative phasing on individual modes, between the analytical and numerical representations, can differ by a factor of − 1 (recall that the eigenfunctions and eigenvectors are unique only to a signed constant), and yet both representations are completely valid.

Consider obtaining a coupling matrix $\boldsymbol{C}$ for a given set of eigenfunctions or eigenvectors with relative phasing, defined as + 1, such that all terms in $\boldsymbol{C}$ are positive. Now if the relative phase of the ith eigenfunction or eigenvector is changed to − 1, then the diagonal term C_{ii} will still be positive, but all off-diagonal terms C_{ix} and C_{xi} will be negative. If the relative phase of the ith and jth eigenfunction or eigenvector is changed to − 1, then C_{ii} and C_{jj} will still be positive, but all terms C_{ix}, C_{xi}, C_{jx}, and C_{xj} will be negative, except for C_{ij} and C_{ji}, which will be positive. But this variation in the sign of the coupling matrix with respect to phasing does not invalidate the technique presented here. The coupling matrix is generated with respect to a given relative phasing between the eigenfunctions or eigenvectors. As long as consistent relative phasing is maintained in all analyses, in particular, the modal expansion, Eq. (34), then the ultimate results will be independent of the relative phasing.

Table 4 compares the relative phases of the modes obtained from the analytical analysis to those obtained from the finite element analysis, for Figs. 4 and 5. For the analytical modes the relative phase of all of the modes is + 1. For the numerical modes the relative phase varies as either + 1 or − 1. Given this relative phasing, the signs of the elements of the numerically obtained coupling matrix clearly follow the behavior discussed earlier.

To explain the divergence between the analytical results and the numerical results, consider Figs. 4 and 5 again. Note that the mode shapes of the higher-order numerical modes exhibit a divergence in shape compared to those of the analytical modes. This divergence in the mode shape causes the discrepancy in the higher-order elements of $\boldsymbol{C}$.

Conclusion

The technique presented in this paper permits the extraction of acoustic intermodal coupling information from numerically modeled, baffled planar structures. The technique generates results in close agreement to a parallel analytical development. Below the coincidence wave number ratio, the intermodal coupling effects cannot be neglected with respect to the total radiated power. Indeed, it is quite possible that the intermodal coupling generates more output acoustic power than individual independent modes. Above the coincidence wave number ratio, the intermodal coupling is insignificant compared to the self-radiation; thus, the modes can be treated independently.

The numerical techniques and tools developed here are readily extendable to other geometries and structures. For example, the boundary element method could be used to generate an expression analogous to Eq. (30) for a three-dimensional structure. A finite element analysis of the same structure could then be used to determine the modes of the structure and, through Eq. (36), the modal interactions. This provides a means of quantifying such effects for structures without analytical modes for either three-dimensional or planar structures.

Acknowledgments

A portion of this research was conducted while the author was at the Technical University of Berlin, Institute of Technical Acoustics, while the author was supported by the Acoustical Society of America's F. V. Hunt Postdoctoral Fellowship. The author thanks M. Heckl, Director of the Institute of Technical Acoustics, for his support and encouragement during this Fellowship year. The author gratefully acknowledges the assistance of Koorosh Naghshineh, at the Center for Acoustics and Vibration, Pennsylvania State University, for providing the code used to develop the discrete numerical representation.

References

[1]Skudrzyk, E., *Simple and Complex Vibratory Systems,* Pennsylvania State University Press, University Park, PA, 1968, p. 409.

[2]Reddy, C. V. R., "Response of Plates with Unconstrained Large Damping Treatment To Random Acoustic Excitation," *Journal of Sound and Vibration,* Vol. 69, No. 1, 1980, pp. 35–45.

[3]Davies, H. G., "Low Frequency Random Excitation of Water-Loaded Rectangular Plates," *Journal of Sound and Vibration,* Vol. 15, No. 1, 1971, pp. 107–126.

[4]Davies, H. G., "Sound from Turbulent-Boundary-Layer-Excited Panels," *Journal of the Acoustical Society of America,* Vol. 49, No. 3, 1971, pp. 878–889.

[5]Yousri, S. N., and Fahy, F. J., "Acoustic Radiation by Unbaffled Cylindrical Beams in Multimodal Transverse Vibration," *Journal of Sound and Vibration,* Vol. 40, No. 3, 1975, pp. 299–306.

[6]Keltie, R. F., and Peng, H., "The Effects of Modal Coupling on the Acoustic Power Radiation from Panels," *Transactions of the ASME, Journal of Vibration, Acoustics, Stress and Reliability in Design,* Vol. 109, No. 1, 1987, pp. 48–54.

[7]Wallace, C. E., "Radiation Resistance of a Baffled Beam," *Journal of the Acoustical Society of America,* Vol. 51, No. 3, 1972, pp. 936–945.

[8]Levine, H., "On the Short Wave Acoustic Radiation from Planar Panels or Beams of Rectangular Shape," *Journal of the Acoustical Society of America,* Vol. 76, No. 2, 1984, pp. 608–615.

[9]Deffayet, C., and Nelson, P. A., "Active Control of Low-Frequency Harmonic Sound Radiated by a Finite Panel," *Journal of the Acoustical Society of America,* Vol. 84, No. 6, 1988, pp. 2192–2199.

[10]Baumann, W. T., Saunders, W. S., and Robertshaw, H. S., "Active Suppression of Acoustic Radiation from Impulsively Excited Structures," *Journal of the Acoustical Society of America,* Vol. 90, No. 6, 1991, pp. 3202–3208.

[11]Pan, J., Snyder, S. D., Hansen, C. H., and Fuller, C. R., "Active Control of Far-Field Sound Radiated by a Rectangular Panel—A General Analysis," *Journal of the Acoustical Society of America,* Vol. 91, No. 4, 1992, pp. 2056–2066.

[12]Fuller, C. R., and Burdisso, R. A., "A Wavenumber Domain Approach to the Active Control of Structure-Bome Sound," *Journal of Sound and Vibration,* Vol. 148, No. 2, 1991, pp. 355–360.

[13]Fuller, C. R., "Active Control of Sound Transmission/Radiation from Elastic Plates by Vibration Inputs: I. Analysis," *Journal of Sound and Vibration,* Vol. 136, No. 1, 1990, pp. 1–15.

[14]Fuller, C. R., "Experiments on Reduction of Propeller Induced Interior Noise by Active Control of Cylinder Vibration," *Journal of Sound and Vibration,* Vol. 112, No. 2, 1986, pp. 389–395.

[15]Fuller, C. R., Metcalf, V. L., Silcox, R. J., and Brown, D. E., "Experiments on Structural Control of Sound Transmitted Through an Elastic Plate," *Proceedings of the 1989 American Control Conference* (Pittsburgh, PA), Vol. 3 of 3, IEEE Service Center, Piscataway, NJ, 1989, pp. 2079–2084.

[16]Rogers, C. A., Fuller, C. R., and Liang, C., "Active Control of Sound Radiation from Panels Using Embedded Shape Memory Alloy Fibers," *Journal of Sound and Vibration,* Vol. 136, No. 1, 1990, pp. 164–170.

[17]Rogers, C. A., Liang, C., and Fuller, C. R., "Modeling of Shape Memory Alloy Hybrid Composites for Structural Acoustic Control," *Journal of the Acoustical Society of America,* Vol. 89, No. 1, 1991, pp. 210–220.

[18]Meirovitch, L., and Thangjitham, S., "Active Control of Sound Radiation Pressure," *Transactions of the ASME, Journal of Vibration, Acoustics, Stress and Reliability in Design,* Vol. 112, No. 2, 1990, pp. 237–244.

[19]Pierce, A. D., *Acoustics: An Introduction to Its Physical Principles and Applications,* Acoustical Society of America, Woodbury, NY, 1989, pp. 213, 214.

[20]Cunefare, K. A., "The Minimum Multimodal Radiation Efficiency of Baffled Finite Beams," *Journal of the Acoustical Society of America,* Vol. 90, No. 5, 1991, pp. 2521–2529.

[21]Naghshineh, K., *Strategies for the Optimum Design of Quiet Structures: Use of Material Tailoring and/or Active Vibration Control,* Ph.D. Dissertation, Pennsylvania State Univ., University Park, PA, 1991.

[22]Shames, I. H., and Dym, C. L., *Energy and Finite Element Methods in Structural Mechanics,* Hemisphere, Washington, D.C., 1985, Chap. 11, 16.

[23]Meirovitch, L., *Computational Methods in Structural Dynamics,* Sijthoff & Noordhoff, Rockville, MD, 1980, pp. 364, 365.

[24]Cunefare, K. A., and Koopmann, G. H., "Acoustic Design Sensitivity for Structural Radiators," *Transactions of the ASME, Journal of Vibration and Acoustics,* Vol. 114, No. 2, 1992, pp. 178–186.

[25]Smith, D. C., and Bernhard, R. J., "Computation of Acoustic Shape Design Sensitivity Using a Boundary Element Method," *Transactions of the ASME, Journal of Vibration and Acoustics,* Vol. 114, No. 1, 1987, pp. 127–132.

[26]Maidanik, G., "Response of Ribbed Panels to Reverberant Acoustics Fields," *Journal of the Acoustical Society of America,* Vol. 34, No. 6, 1962, pp. 809–826.